Kick Stability Analysis of the LHC Inflectors

M.J. Barnes, G.D. Wait, TRIUMF,

L. Ducimetière, U. Jansson, G.H. Schröder, E.B. Vossenberg, CERN SL Division

Abstract

Two sets of four LHC inflector magnet systems must produce a kick of 1.36 Tm each with a duration of 6.5 μs, a rise time of 750 ns, and an overall stability of ± 0.5 %. The electrical circuit of the complete system, including all known stray quantities, has been simulated with PSpice. Many stray elements were determined from Opera2D simulations which included eddy-currents. 3D analyses have also been carried out for the kicker magnet using the electromagnetic analysis code Opera3D. Equivalent circuits which simulate the frequency dependence of inductance and resistance of the Pulse Forming Network (PFN) have been derived. The dimensions of the PFN coil have been selected to give the correct pulse response. The end cells of the PFN have also been optimised. The discharge stability of various PFN capacitors has been measured. This paper presents the results of both the analyses and measurements.

1 SIMULATIONS

A previous paper by the authors[1] details operational requirements, geometry, and results of initial PSpice simulations, for the PFN. The research reported in the present paper builds on that presented previously.

1.1 PFN Coil

The PFN consists of two $10\,\Omega$ L-C networks of 27 cells connected at both ends in parallel. The ends are equipped with thyratron switches, the main switch (MS) at the magnet side and the dump switch (DS) on the opposite end. Each PFN coil has a diameter of 42.4 mm and is precision wound as a continuous straight solenoid with a constant pitch of 22 mm, to assure the same self inductance and mutual coupling coefficients for all cells, apart from the end cells. The coil conductor is a Cu tube of 8 mm diameter and 1 mm wall thickness. The inner cell inductances are composed of 7 turns. Each coil is surrounded by a 1.5 mm thick Omega shaped copper screen which has an internal radius of 140 mm (Fig. 1). Both PFNs are mounted in a rectangular tank with walls made of 5 mm thick mild steel.

The inductance and resistance of each cell exhibit a strong frequency dependence that has been quantified with the simulation code Opera2D[2]. The total inductance of a cell decreases by approximately 13 % between 0.1 Hz and 40k Hz (Fig. 2), hence the radius of the coil cannot be based on the DC value of inductance. In order to extract both self and mutual inductance, as a function of frequency, from the Opera2D predictions, the simulations were carried out in four steps on 10 consecutive central cells of 7 turns each:

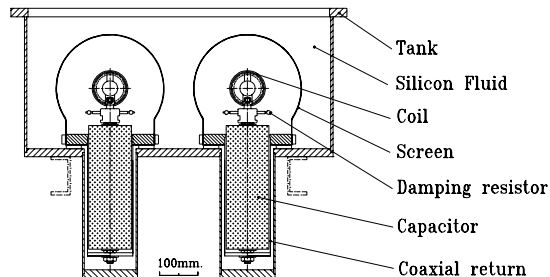1. one cell is modelled as carrying current;

Figure 1: Cross-section of $5\,\Omega$ PFN

2. three cells carry current: there is one off-state cell between adjacent on-state cells;
3. three adjacent cells carry current;
4. all cells carry current.

Predicted stored energy permits the calculation of various quantities. The first step gives the self-inductance per cell. The combination of the first and second steps give the mutual coupling coefficient k_{13} between cell inductances 1 and 3, provided that k_{15} can be neglected. The first, second and third steps then give k_{12}. As a cross-check the total inductance per cell (self and mutual) calculated from steps 1 through 3 is compared with that calculated from step 4. Steps 1 through 4 are carried out over a range of frequencies from 0.1 Hz to 10 MHz. The predictions at 0.1 Hz have been checked with DC simulations from Flux2D[3] and calculations based on equations in Grover[4], with the screen assumed to be at infinity, and are in excellent agreement.
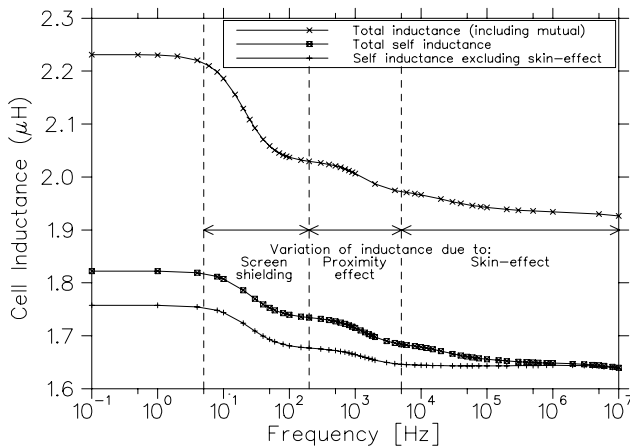

Figure 2: Inductance of standard cell versus frequency

Fig. 2 shows three plots of cell inductance as a function of frequency (see legend), as calculated from Opera2D simulations. The curves can be split approximately into four frequency bands. Below 5 Hz magnetic field is present outside the copper screen resulting in a high inductance. Between approximately 5 Hz and 200 Hz there is a significant de-
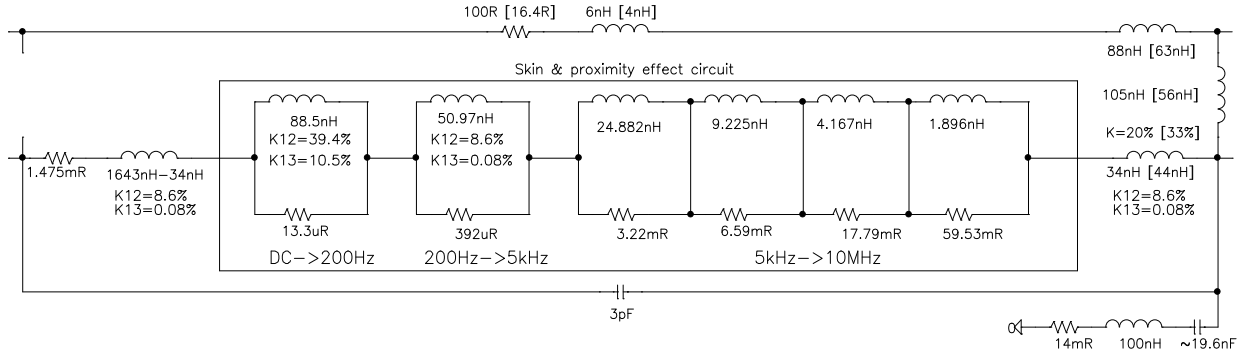
Figure 3: Equivalent circuit for a 7 turn cell [damping circuit values for MS end cell in parentheses]

crease in both self-inductance and the mutual coupling coefficients because eddy currents induced in the screen result in negligible field outside of the screen. Between 200 Hz and 5 kHz the reduction of inductance is mainly due to the proximity effect. Above 5 kHz the main cause of variation of cell inductance can be attributed to skin-effect.

Fig. 3 shows the equivalent circuits utilised to simulate the cell resistance and inductance over various frequency ranges. The simulated values associated with the damping circuit of the MS end cell, are shown in square parentheses. The PSpice Optimizer[5] has been utilised to fit the equivalent circuit to the Opera2D predictions. The maximum error for the equivalent inductance and resistance values is 1.5 % and 0.1 %, respectively up to a frequency of 8 MHz. PSpice transient analyses show that the variation of cell resistance and inductance below 200 Hz, i.e. the effect of the mild-steel tank, has negligible effect: thus this section of Fig. 3 can be eliminated from the model.

The frequency dependent losses result in a droop of the 'flat-top' field[1]: a similar slope is produced by replacing the skin and proximity effect circuits of Fig. 3 by a resistor, whose value corresponds to the cell resistance at approximately 40 kHz. The losses can be compensated for by linearly grading the cell capacitors such that they increase in value from the MS end to the DS end of the PFNs[1]. The optimum grading is 0.09 % per cell. Measurements confirm that the natural spread in capacitance values of production batches is sufficient to achieve the required grading.

Each capacitor has an equivalent series resistance of approximately 14 mΩ. In addition the end to end stray capacitance associated with a cell is approximately 3 pF (Fig. 3). PSpice transient analyses carried out with these stray values show that they have negligible effect upon the predicted magnetic field.

1.2 End-cell Inductance

The PSpice Optimizer has been used to independently optimize the inductance of both the MS and DS end cells. The value of the MS end cell inductance was specified, and then the Optimizer was run with the values of the front and MS cell[1] as parameters, and both rise-time and ripple were included in the specifications. Provided that the rise-time and

ripple definitions were achieved, the rise-time was reduced and the Optimizer re-run. The minimum field rise-time occurs for a self-inductance of approximately 130 % of that of a central cell, and remains within 10 ns of the minimum for an inductance in the range of 122 % to 135 %. A nine turn cell has been chosen, as it has a self-inductance of approximately 133 %. Opera2D simulations show that the corresponding k_{12} coupling factor to the adjacent cell is 7.4 % (compared with 8.6 % between two adjacent central cells). A similar analysis for the DS end results in a 5 turn cell: the self inductance is 67 % of the central inductance. The coupling coefficient k_{12} to the adjacent cell is 10.3 %.

1.3 Damping Circuit

Each cell of the PFN has a damping resistor, connected in parallel with the coil inductance, to damp out flat-top oscillations[1]. The nominal values of the damping resistor are $16.4\,\Omega$ for the DS end cell and $100\,\Omega$ for the other cells. The damping circuit self and mutual inductance terms are calculated using both Opera2D and Grover[4], and are shown in Fig. 3. The stray inductance is simulated as a self-inductance (88 nH) mutually coupled (k=20 %) to the coaxial portion of the self-inductance (34 nH) of the associated PFN cell. There is also inductance associated with the wiring connections (105 nH) to the PFN winding, and the internal inductance of the resistors (6 nH). Due to the relatively large value of the damping resistor associated with the central and DS end cells, their stray inductances have negligible effect upon the predicted magnetic field. However the stray inductance associated with the damping circuit of the MS end cell can cause a significant overshoot and subsequent ripple of the magnetic field. For this reason, two parallel resistors, one on either side of the coil (Fig. 1), are required for the MS end cell.

1.4 Simulation Results

Fig. 4 shows the predicted magnetic field in the kicker magnet for a PFN built as described above. End effects in the magnet are neglected, and the terminators and cables are simulated as being ideal. The rise and fall times (0.1 % to 99.9 %) are 641 ns, and 2.8 μs respectively for a (reduced) pulse width of 4.25 μs. A study of the post-pulse field shape
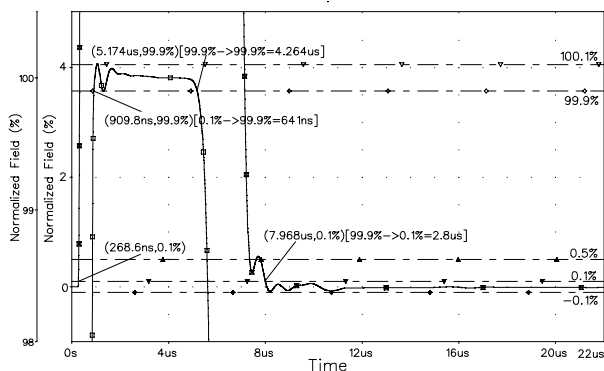
Figure 4: Predicted field in kicker magnet

as a function of pulse width predicts that for widths of 4 μs, 4.5 μs, 5 μs and 6 μs, the field fall time (99.9 % to 0.1 %) is 2.8μs, 2.8 μs, 4.2 μs and 4.9 μs, respectively. The predicted fall-time is less than 3 μs, for all the above pulse-widths, if a fall-time definition of 99.9 % to 0.3 % is used.

2 COMPONENT STABILITY

2.1 Discharge stability of PFN capacitors

Previous experiences have shown that contact problems inside PFN capacitors can be one of the main sources of flat-top degradation. Several technologies of capacitor fabrication, from various manufacturers, have thus been investigated. A stability test has been set up, in which the capacitor under test is discharged from 15 kV into a 10 Ω resistive load through a single gap thyratron. The discharge current was monitored over a few thousands cycles. During part of the test the capacitors were subjected to knocks and vibrations. The overall stability of the power supply was limited to ±0.25 %. The test capacitors differed by the method of internal connection between the elementary series-connected units which compose each capacitor. Capacitors type 1 had elementary units only pressed together and maintained by an insulating rod; capacitors type 2 were identical but had an additional spring to ensure a good contact pressure; capacitors type 3 and 4 from two different manufacturers were composed of elementary units soldered together.

The following results were obtained: capacitors type 1 had an instability of ±0.35 % which increases to ±0.95 % when subject to knocks and vibrations; for capacitors of type 2 the instability was ±0.35 % and ±0.40 %, respectively. Capacitors type 3 and 4 have shown an instability of ±0.25 %, independent on whether knocks and vibrations were applied. From these values, the instability of the power supply itself must be deducted. The results confirm that internal elementary units must be soldered together to achieve an acceptable stability.

2.2 Stability of termination resistors

For both main and dump resistors, existing coaxial high voltage, low inductance subassemblies will be used. They are composed of 10 series stacked ceramic carbon discs, immersed in a forced liquid silicone flow and cooled by water. The long term stability of the unit is linked to the ageing of the resistor discs. The relative resistance change based on manufacturer tests[6] can be expressed in the empirical relation dR(%)=5.6(1-exp(-t/20)), where t is the time in weeks. According to this formula, the 0.1 % stabilisation of the final resistance value is reached after about 80 weeks. In order to accelerate the stabilisation process, CERN already pre-impregnates the discs under vacuum and high temperature, but further investigations remain to be made.

The short term stability is linked to the temperature coefficient of the material (-0.08 %/$^\circ$C). Each PFN pulse has a maximum energy of 1730 J and will heat up the resistor stack by 0.2°C. Without heat exchange, the temperature would increase by 2.2°C between the 1st and 12th pulse, leading to a resistance decrease of 0.18 %. A test is underway to measure the capability of the forced cooling system to reduce the resistance variation. Care will also be required to guarantee the initial temperature of the resistor stacks to within 1°C before each injection period.

3 CONCLUSION & OUTLOOK

Beam emittance conservation during injection into the LHC imposes stringent design requirements on the flat-top ripple of the magnetic field of the injection kicker systems. In order to establish a realistic equivalent circuit of the system for pulse response simulations, secondary effects such as frequency dependence of the PFN coil and damping resistors as well as stray elements have been incorporated. The results show that the required pulse response performance can be achieved. Further refinements to the model are required, and then a sensitivity analysis will be performed. In parallel the pulse to pulse stability of discharge capacitors has been analysed resulting in the conclusion that all internal capacitor elements must be connected by soldering.

4 REFERENCES

[1] Ducimetière L., Jansson U., Schröder G.H., Vossenberg E.B., CERN SL Division, Barnes M.J., Wait G.D., TRIUMF, "Design of the Injection Kicker Magnet System for CERN's 14 TeV Proton Collider LHC", Tenth IEEE International Pulsed Power Conference Albuquerque, June 1995.

[2] Vector Fields Ltd., 24 Bankside, Kidlington, Oxford. OX5 1JE. UK. Tel. 0867 570151.

[3] CEDRAT S.A., ZIRST 4301, 38943 Meylan Cedex, France. Tel. (33) 76 90 50 45.

[4] Grover, Frederick W., "Inductance Calculations: Working Formulas and Tables", Special edition prepared for Instrument Society of America, 1973. Originally published: New York: Van Nostrand, 1946.

[5] MicroSim Corporation, 20 Fairbanks, Irvine, California 92718. USA. Tel (714) 770 3022.

[6] HVR International Ltd, Bede Industrial Estate, Jarrow Tyne & Wear, NE32 3EN, England.